P178

Short Wavelength Infrared Imaging Impacts on Storm Spotting: A Pilot Study

Matthew O. Seedorf and Robin L. Tanamachi,
Purdue University, West Lafayette, Indiana

1. Introduction

Since the National Weather Service (NWS) SKYWARN program began in the 1970s, it has been one of the key tools in helping to improve the accuracy and timing of tornado warnings (Doswell et al. 1999). One factor that has impeded storm spotters throughout the years is observing a thunderstorm or tornado in low visibility conditions (e.g., in dense haze, or at night).

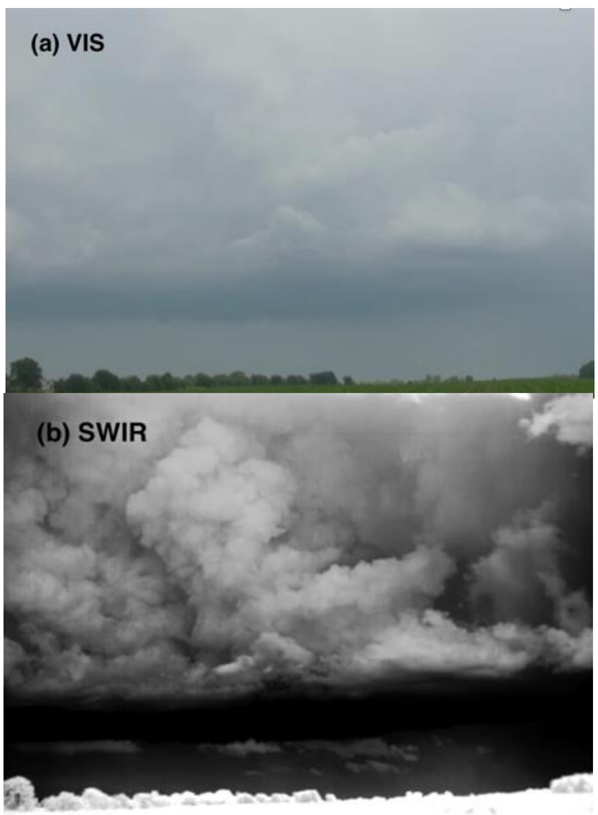

Fig. 1. A side-by-side comparison of (a) VIS and (b) SWIR images of the same thunderstorm cloud base near Lebanon, Indiana on 15 June 2016, showing the higher dynamic range and enhanced cloud texture details in the SWIR image.

In this pilot study, we explore the use of shortwave infrared (SWIR, 0.9 – 1.6 μm) imagery in observing thunderstorms, and compare the SWIR images of thunderstorm cloud bases to visible-wavelength (VIS) images, which serve as a proxy for in-person storm observations. SWIR imagery typically has a higher dynamic range in haze and low-light conditions owing to its use of longer wavelengths than visible light (e.g., Fig. 1). The overarching goal is to determine if the SWIR imagery could help improve detection of poorly-visible tornadoes in supercells (i.e., those obscured by haze or darkness). We present a methodology, built on existing storm observation techniques, for safely imaging severe thunderstorm cloud bases using a SWIR camera. We also present preliminary results of an eye tracking study in which SWIR and VIS video footage of thunderstorm cloud bases were shown to trained weather spotters. It is our hope that the use of eye tracking technology will help us more objectively assess whether the trained spotters are better able to detect pretornadic cloud features in the SWIR images.

2. Methodology

Fig. 2: The Canon HV30 HD camcorder (left on tripod) and the Goodrich GA 1280J SWIR camera (right) recording video in the 7 July 2016 Boswell, Indiana storm.

During spring 2016, a SWIR imaging camera and digital video recorder (DVR) were used to image storms. The two video cameras

Table 1: The date, time in UTC, nearest town location in miles, and conditions observed of the SWIR and VIS camera.

Date	**Time (UTC)**	**Nearest Town Location**	**Conditions observed**
06/15/16	1945 to 1955	9.2 km (5.7 mi) ENE Jamestown, IN	Multicell storms with lowered cloud bases
06/15/16	2000 to 2045	3.2 km (2.0 mi) S Lebanon, IN	Outflow-dominated clusters with precipitating rain shafts, and bubbling cumulonimbus clouds
07/07/16	2345 to 0000	11 km (7.0 mi) N Boswell, IN	Rain shafts in multicell clusters
07/08/16	0022 to 0030	4.8 km (3.0 mi) N Kentland, IN	Rain shafts, rainbow
07/08/16	0100 to 0115	4.0 km (2.5 mi) mi S Wolcott, IN	Scud clouds with weak rotation
07/13/16	2125 to 2200	3.5 km (2.2 mi) W Belgium, IL	Cumulus towers, rain shafts, lowered cloud base

were mounted side-by-side on a dual camera mount (Fig. 2). The VIS video camera (left camera in Fig. 2) was a Canon Vixia HV30 high-definition (HD) camcorder equipped to record in 1080/60i HD. The focus on the VIS video camera was set to infinity in order to record details of distant cloud features.

The SWIR video camera (right camera in Fig. 2) was a Goodrich GA 1280J Enclosed Indium Gallium Arsenide (InGaAs) High Resolution SWIR camera. The camera stabilizes the focal plane array temperature and produces a video signal digitalized with a resolution of 12 bits using an analog-to-digital converter. The SWIR camera is sensitive to wavelengths between 0.7 μm to 1.7 μm. The digital video signal was recorded by a Churchill Navigation ION DVR.

During June and July 2016, weather forecasts for the Midwest U.S. were monitored daily. When conditions for severe weather were possible within a 100-mile radius of West Lafayette, Indiana, deployment of the two cameras would then occur. National Weather Service (NWS) Doppler radar (WSR-88D) observations were interrogated in real time using commercial software (such as RadarScope and GR2Analyst) to ensure safe deployment conditions for the camera, and assess the presence or absence of low-level rotation in observed storms. Dual camera deployments occurred on a total of six days (Table 1).

The VIS and SWIR videos were then edited using Adobe Premiere Pro software, and synchronized in time to within less than one second. The videos were then matched up in a side by side view (e.g., Fig. 1), with their fields of view matched as closely as possible. SWIR video brightness was increased up to 35% in order to improve the contrast. The video was partitioned into clips ranging in length from 30 seconds to two minutes.

Fig. 3: A trained spotter participant observing VIS video footage of a developing tornado while using the Tobii TX300 eye tracking system. The spotter's eyes are tracked by a low-power, infrared sensing array mounted below the screen.

A subset of the VIS and SWIR video clips where then shown to two trained weather spotters with similar experience levels (1.5 and two years since NWS training, respectively) using a commercially available eye tracking machine (Fig. 3). According to Bowden et al. (2016), exploring a forecaster's eye movements while looking at radar data may enrich our understanding of their cognitive decision making processes when issuing warnings.

Our approach to the use of the eye tracking technology was similar to that of Bowden et al. (2016), in that we focus on two measures: fixation count and fixation duration. This study is novel in that we are applying a different type of imagery (SWIR and VIS video) to a different population group (trained storm spotters) to assess their decision making process in a different application (visual detection of tornadoes). The principal question we seek to address is: Do eye gaze fixations on cloud features in the SWIR video differ significantly from eye gaze fixations on a VIS video of the same scene?

The trained spotters' eye gaze data was collected using the Tobii TX300 eye tracking system (Fig. 3). The system is able to track and measure a subject's eye fixations on a computer monitor, on which the VIS and SWIR videos were displayed. Proprietary Tobii Studio 3.3 software was used to provide data visualization, and statistical metric calculations.

The spotter sat in front of the TX300 system (Fig. 3), where an infrared detection system could trace the spotter's pupils and retina glint as they looked at objects on the screen (Olsen, 2012). The spotters were first *both* shown a VIS video of the developing 23 May 2016 Woodward, Oklahoma tornado (Fig. 4) in order to gauge their eye fixations on a known tornado event. Each participant was then shown a side-by-side VIS and SWIR video clip of a non-tornadic cloud base (Fig. 1) in order to familiarize him or her with the different appearance of SWIR video.

The spotter was then shown a series of either VIS or SWIR video clips cloud base features, and his or her eye movements were recorded. If Participant 1 saw a VIS clip of a scene, Participant 2 was shown the corresponding SWIR clip, and vice versa. The video clips were then replayed to the participant with the eye fixations overlaid, and the participant was asked to retrospectively recall their thoughts about whether each scene showed any features worth reporting to the NWS.

This study focused on two sets of data that the TX300 produces: the heat map and gaze plot. Both types of plots represent fixation and fixation duration on the screen in slightly different ways. In a heat map, the fixation counts are normalized by the maximum number of fixations over the entire field of view, with brighter colors representing areas where the eyes fixated more frequently. The gaze plot shows a series of points where the subject fixated; the longer the eye fixated on a point, the larger the corresponding circle will be on the gaze plot. These two plots were then analyzed for each clip to determine if significant eye movement differences occurred between the VIS and SWIR images.

3. Results

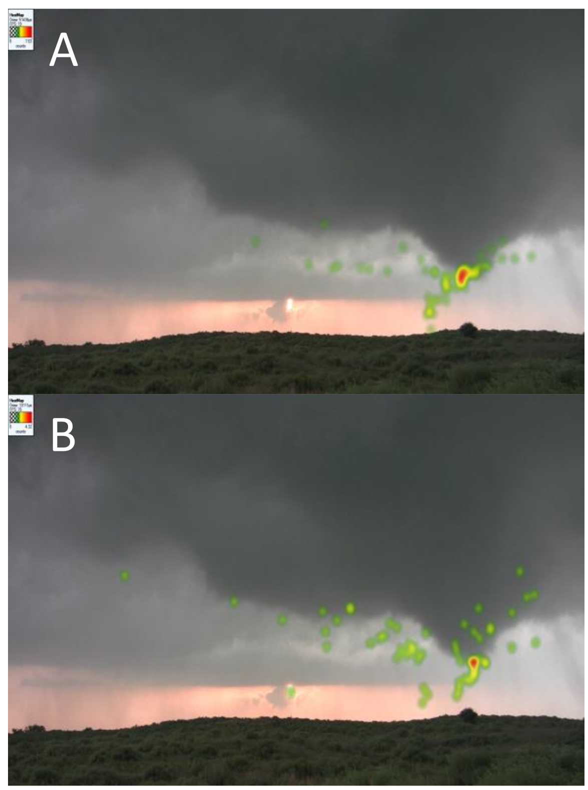

Fig. 4: Heat maps for the Woodward, Oklahoma tornado video clip for (a) Participant 1 and (b) Participant 2, showing the normalized fixation count for the scene.

As a control, the participants were shown the *same* VIS video of the developing 23

May 2016 Woodward, OK tornado. Fig. 4 shows the heat maps generated by each participant from this 1-minute VIS video clip. Both participants fixated on the developing funnel cloud, showing that they both had been properly trained to identify and track pretornadic cloud base features. Next, each participant was shown a video clip of the 7 July 2016 Boswell non-tornadic storm (Table 1). Participant 1 was shown the SWIR version of this video (Fig. 5a), while Participant 2 was shown the VIS version (Fig. 5b) Both participants were able to locate the cloud base in the storm, however, Participant 1 focused more on the right side of the video clip away from the rain shaft, while Participant 2 focused more on the rain shaft itself. In this particular clip, the cloud base was more easily discerned in the VIS video than the SWIR video, as evidenced by the higher fixation count along the cloud base in the VIS video (Fig. 5b).

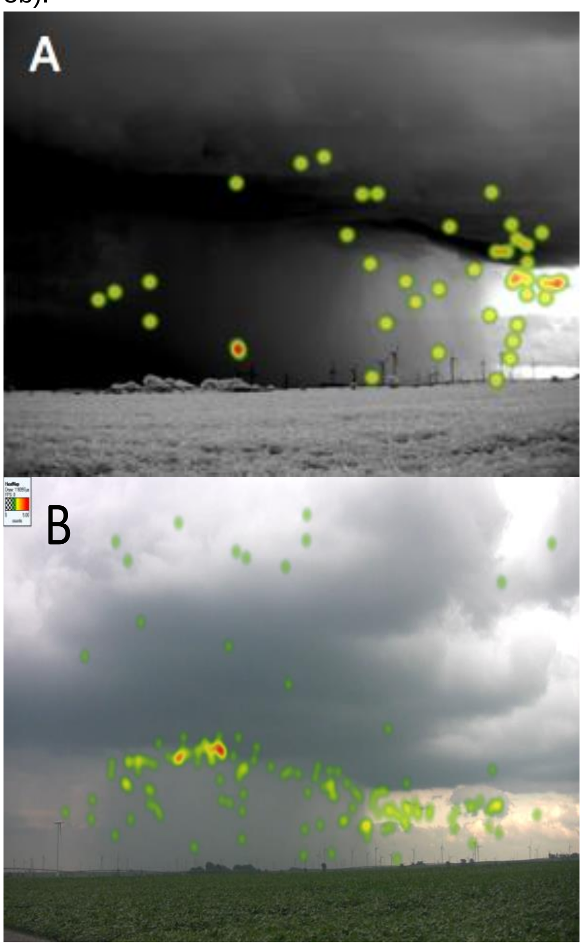

Fig. 5: (a) SWIR and (b) VIS images of the Boswell, Indiana storm of 7 July 2016, overlaid with the eye fixation heat map for (a) Participant 1 and (b) Participant 2.

For the 13 July 2016 Belgium, IL storm, Participant 1 was again shown the SWIR footage (Fig. 6a), while Participant 2 was shown the VIS footage (Fig. 6b). Both scenes show a nonrotating cloud base in the foreground, which both participants studied briefly before fixating on the more distant cloud base on the horizon. In this case, no significant differences were found in the heat maps generated from the SWIR and VIS video.

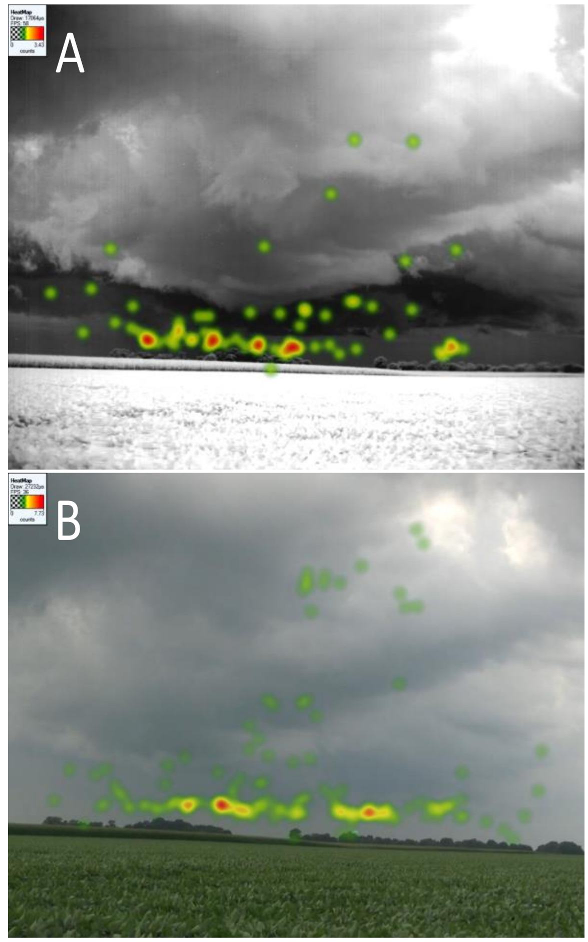

Fig. 6: (a) SWIR and (b) VIS images of the 13 July 2016 Belgium, Illinois storm, overlaid with eye fixation heat maps for (a) Participant 1 and (b) Participant 2.

The final clip shown to the participants again featured a cloud base observed in the 13 July 2016 Belgium, IL storm. In contrast to the previous two clips, Participant 1 (Participant 2) viewed the scene in VIS (SWIR) imagery. Both VIS and SWIR imagery showed a distant, ambiguous, conical lowering in the cloud base (Fig. 7). As Participant 1 viewed the VIS imagery (Fig. 7a, b), he or she focused on the ambiguous conical lowering for nearly the entire duration of

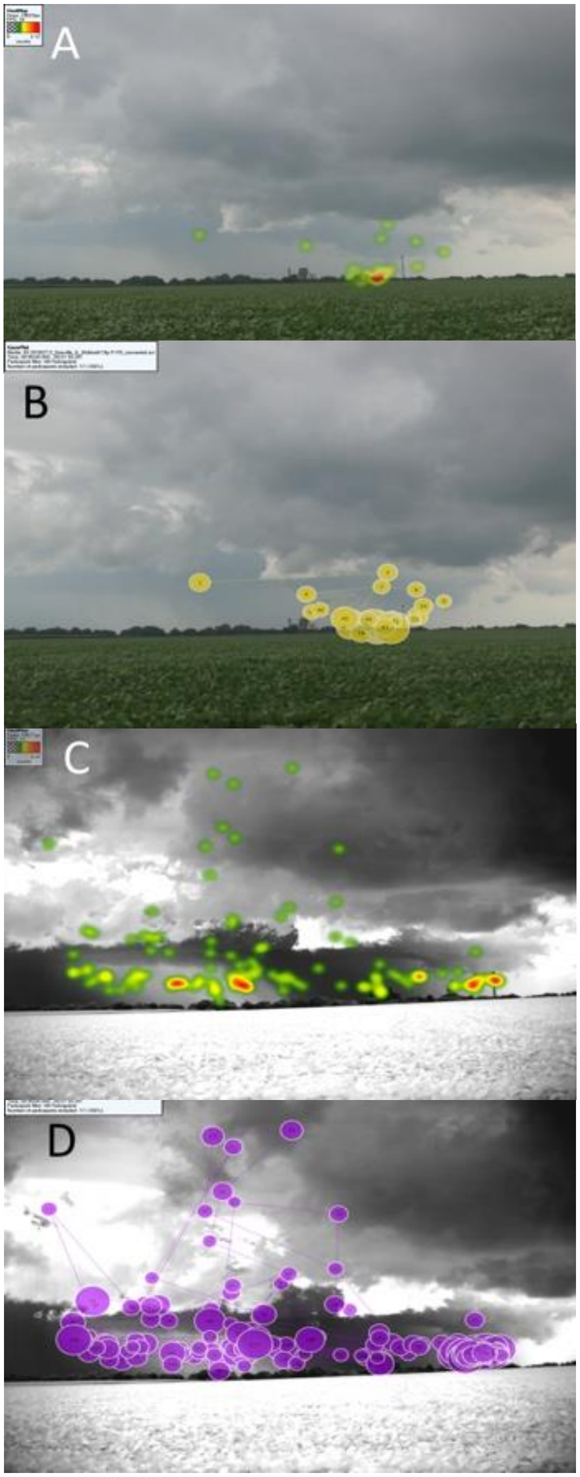

Fig. 7: (a and b) VIS and (c and d) SWIR images of the 13 July 2016 Belgium, Illinois storm, overlaid with eye fixation heat maps for (a) Participant 1 and (c) Participant 2 can gaze plot maps for (b) Participant 1 and (d) participant 2. In panels (b) and (d), the individual circles represent a series of eye fixations, numbered in chronological order, and the circle size is proportional to the fixation duration

the clip (2 min). During his retrospective recall, Participant 1 mentioned that he thought it was a possible funnel cloud, but wasn't sure until the end of the video that it was non-tornadic. Participant 2 viewed this scene in SWIR imagery but the associated gaze plot and heat map (Fig. 7c, d), showed that Participant 2 had no general focus for the duration of the video. During the retrospective recall, Participant 2 said that he or she was able to dismiss the ambiguous conical feature very early, because the feature was clearly just a scud cloud generated by outflow. Participant 2 also mentioned being overwhelmed at the information content of this particular SWIR video, but it had no effect on the identification of the scud cloud.

4. Discussion

Overall, the use of SWIR imagery was shown in this pilot study to affect the way in which storm spotters interrogated and perceived the same cloud base. The final clip (Fig. 7), showing the ambiguous conical lowering, stood out. Participant 2, viewing the SWIR video, was able to identify the feature as a scud cloud within a few seconds, while Participant 1, viewing the VIS video, fixated on the feature for nearly two minutes to be certain it wasn't a funnel cloud. The use of the SWIR imagery in this instance significantly changed the manner in which the two participants interrogated the scene, and while both came to the same conclusion (i.e., the feature was not a funnel cloud), Participant 2 reached that conclusion much more quickly using the SWIR imagery.

5. Conclusion

In this pilot study, we developed a methodology to image storms safely using a SWIR camera, and showed that trained storm spotters interrogate images of a cloud base differently depending on whether they are viewing the scene in VIS or SWIR light. **We conclude that there is a distinct possibility that SWIR video imagery can be beneficial to storm spotters.** In particular, an ambiguous, nontornadic cloud base lowering was quickly dismissed by a participant viewing the scene in SWIR, while a participant viewing the same scene in VIS light had a more difficult time determining that the feature was nontornadic. SWIR light is less susceptible to scattering by intervening haze, allowing cloud base features to be more easily discerned.

Further study of SWIR imagery augmentation on storm spotting is warranted. This pilot study only utilized SWIR video of nontornadic storms, and only two participants were recruited. In the future, we hope to enlarge our database of available SWIR storm video to include tornadoes and other severe weather phenomena, and simultaneously recruit a much larger population of trained spotters to participate in the eye tracking study.

Acknowledgements

Special thanks to Curt Dvonch of Sensors Unlimited, Inc. for the use of the SWIR camera, and to Tom Churchill of Churchill Navigation for the use of the DVR. Access to the Tobii TX300 eye tracking system and its associated software were provided by the Purdue Discovery Learning and Research Center; training was provided by Deborah Steffen. Purdue students Justin Buckingham and Will Smith served as the volunteer participants for the eye tracking study. Fuel and transportation costs for the video deployments were provided by Purdue University's College of Science. We gratefully acknowledge helpful conversations with Chris Novy and Katie (Bowden) Wilson as we developed this pilot study methodology.

References

Bowden, K., P. Heinselman, and Z. Kang, 2016: Exploring Applications of Eye Tracking in Operational Meteorology Research. *Bull. Amer. Meteor. Soc.*, in press, doi:10.1175/BAMS-D-15-00148.1.

Doswell, C. A., A. R. Moller, and H. E. Brooks, 1999: Storm spotting and public awareness since the first tornado forecasts of 1948. *Wea. Forecasting*, **14,** 544-557.

Olsen, M., 2012: The Tobii I-VT fixation filter: Algorithm description. Accessed 11 July 2016. [Available online at: https://stemedhub.org/resources/2173/download/Tobii_WhitePaper_TobiiIVTFixationFilter.pdf]